SYNTHESIS AND CHARACTERIZATION OF CARBOXYMETHYL CELLULOSE-GLUTARALDEHYDE-La-GRAPHENE COMPOSITE BEADS AND THEIR APPLICATION FOR REMOVAL OF METHYLENE BLUE

ZENGJIN FU,* LEI TAN,* YAN HAO* and TINGRUI LIN**,***

*Institute of Applied Chemistry School of Chemistry and Chemical Engineering, Inner Mongolia University of Science and Technology, Baotou 014010, P. R. China
**Beijing National Laboratory for Molecular Sciences, Radiochemistry and Radiation Chemistry Key Laboratory of Fundamental Science, the Key Laboratory of Polymer Chemistry and Physics of the Ministry of Education, College of Chemistry and Molecular Engineering, Peking University, Beijing 100871, PR China
***Fujian Key Laboratory of Architectural Coating, Skshu Paint Co., Ltd., Putian, Fujian 351100, PR China
✉ Corresponding author: Y. Hao, haoyannk@163.com

Received March 21, 2025

A novel adsorbent was developed through an innovative dual-crosslinking strategy. An environmentally friendly composite adsorbent based on carboxymethyl cellulose (CMC) incorporated with graphene oxide (GO) was prepared for the adsorptive removal of cationic methylene blue (MB). In this method, the synergistic action of La^{3+} and glutaraldehyde was utilized to fabricate carboxymethyl cellulose-glutaraldehyde-La-graphene composite beads (CMC-GA-La-GO) with significantly enhanced adsorption performance compared to its individual components. This paper outlined the synthesis of CMC-GA-La-GO as a straightforward and environmentally benign process. The raw materials were inexpensive and readily available. The resulting CMC-GA-La-GO beads were characterized by FTIR, XRD, TGA and SEM. Furthermore, the parameters associated with the dosage of the adsorbent were also subjected to optimization. The experimental data for the adsorption process were better fitted by the Langmuir model (R^2=0.99), indicating a theoretical maximum adsorption capacity of 113.9 mg·g^{-1}, and were found to follow the pseudo-second-order kinetic model. The gained results demonstrated that the CMC-GA-La-GO could be potentially applied as an effective adsorbent for MB removal from aqueous solutions.

Keywords: carboxymethyl cellulose, graphene oxide, composite, methylene blue, adsorption

INTRODUCTION

Water pollution is frequently associated with human activity and population increase.[1] Synthetic dyes are extensively employed in leather,[2] printing,[3] cosmetics,[4] plastics,[5] and textiles.[6] Considerable amounts of these dyes are often released into the environment without proper treatment, which poses serious or even lethal effects on living organisms.[7] Methylene blue (MB) is an aliphatic hetero base dye, which demonstrates durability against fading when exposed to light, water, oxidizing agents, and microbial environments.[8] Nevertheless, it is extremely toxic, not biodegradable, and poses a considerable threat to human health, along with adverse effects on the environment.[9] The scarcity of high-quality pure water and public health issues necessitate the treatment of printing and dyeing wastewater to safeguard the environment and community well-being.[10]

In recent years, many chemical, physical, and biological methods have been developed and utilized for the treatment of dye wastewater, including methylene blue (MB).[11] Several techniques have been identified for removing MB from wastewater, including adsorption,[12] ion exchange, electrolysis, chemical oxidation,[13] membrane filtration, photodegradation and biodegradation[14] *etc*. Among the aforementioned

strategies, adsorption methods are favored for the removal of contaminating colors in wastewater from industries owing to their cost-effectiveness, straightforward design, operational ease, and high efficiency.[15] From an environmental and economic perspective, bioadsorbents made from biodegradable and sustainable polymers, including cellulose,[16] chitin/chitosan,[17] starch,[18] lignin[19] *etc*., have garnered significant interest.

Cellulose, the most abundant natural polymer among renewable polymers, possesses numerous advantageous properties, such as global availability, renewability, and ease of surface modification. Cellulose exhibits limited water solubility owing to its dense molecular structure, hence constraining its possible applications. Meanwhile, sodium carboxymethyl cellulose (CMC) is a salt derived from the carboxymethylation of natural cellulose. This salt exhibits excellent solubility in aqueous media. Despite its widespread application in wastewater treatment, CMC demonstrates inferior mechanical characteristics and limited adsorption capability. Liu *et al*.[20] aimed to analyze the adsorption behavior of the carboxymethyl cellulose/k-carrageenan/activated montmorillonite composite beads in the adsorption of MB. Under the optimum conditions, the theoretical maximum adsorption capacity of MB was 12.25 $mg \cdot g^{-1}$. To address these constraints, many physical and chemical modification approaches have been utilized for CMC, including crosslinking and grafting.[21-23]

Recent studies have demonstrated that graphene oxide (GO) is an effective material for dye adsorption. This could be attributed to material's optimal two-dimensional structure, exceptional mechanical strength, and comparatively extensive specific surface area. Moreover, it possesses a significant quantity of oxygen-containing functional groups, including carboxyl, hydroxyl, and epoxy groups. GO is hydrophilic, possesses a negative charge, and readily disperses in water to create a stable colloidal suspension.[24] Recently, Yang *et al.*[25] developed a composite hydrogel consisting of graphene oxide and polyacrylamide. Liu *et al.* presented a study on carboxymethyl cellulose sodium/graphene oxide hydrogel microparticles.[26] In their study, the authors demonstrated that the adsorption and mechanical properties of the hydrogels were greatly enhanced by the use of GO.[27,28]

This study utilized CMC and GO as primary synthetic materials to fabricate carboxymethyl cellulose-glutaraldehyde-La-graphene composite beads, designated as CMC-GA-La-GO. Glutaraldehyde (GA) was chosen as the substance that crosslinks to improve the thermal stability of the CMC-GA-La-GO.[29] The composite beads were characterized by FTIR, XRD, SEM, and TGA to assess their structures, morphologies, and thermal stability. MB was chosen as a target pollutant to assess the adsorption characteristics of the adsorbent. The influence of various adsorption conditions on the ability of the absorbent to remove the pollutant was examined. Additionally, adsorption isotherms and kinetic analyses were assessed.

EXPERIMENTAL

Materials

CMC (AR, purity ≥ 99.0%), Lanthanum (III) nitrate hexahydrate ($La(NO_3)_3 \cdot 6H_2O$, AR, purity ≥ 99.0%) and GA (AR, purity ≥ 50.0%) were acquired from Shanghai Macklin Biochemical Co., Ltd. GO was purchased from the Sixth Element (Changzhou) Materials Technology Co., Ltd. MB (AR, purity ≥ 98.5%) was obtained from Tianjin Beilian Fine Chemicals Development Co., Ltd. All reagents used in the experimental procedure were of analytical grade.

Synthesis of materials

The CMC-GA-La-GO was prepared by adding a specific quantity of GO to deionized water and subjecting the mixture to ultrasonic treatment to obtain a homogeneous GO dispersion. A specific quantity of CMC was then added to the GO dispersion and subjected to ultrasonic treatment to form a homogeneous mixture, with a mass ratio of CMC to GO maintained at 1:1. The mixture was subsequently dripped vertically into 0.1 $mol \cdot L^{-1}$ $La(NO_3)_3 \cdot 6H_2O$ solution, resulting in the formation of beads. After 30 minutes, 5.0 mL of GA was introduced to the solution as a crosslinking agent, which was then subjected to thorough agitation. The beads underwent crosslinking at ambient temperature for an additional 24 h, culminating in the creation of CMC-GA-La-GO. The beads were further filtered and washed with deionized water to eliminate any remaining soluble contaminants. Finally, the CMC-GA-La-GO had been successfully synthesized by undergoing a vacuum freeze-drying procedure until it reached a constant weight.

The CMC-GA-La-GO beads were thus obtained through the above procedure. The schematic illustration of the crosslinking and formation process of the CMC-GA-La-GO is shown in Figure 1. Specifically, the bead formation involved a dual-crosslinking mechanism. First, the CMC and GO were interconnected by La^{3+} ions through ionic interactions, leading to the immediate formation of a preliminary three-dimensional network structure upon contact with the La^{3+} solution.[30]

Subsequently, covalent crosslinking was introduced by GA, which reacted with the hydroxyl groups on both CMC and GO to significantly enhance the mechanical and chemical stability of the entire composite.[31]

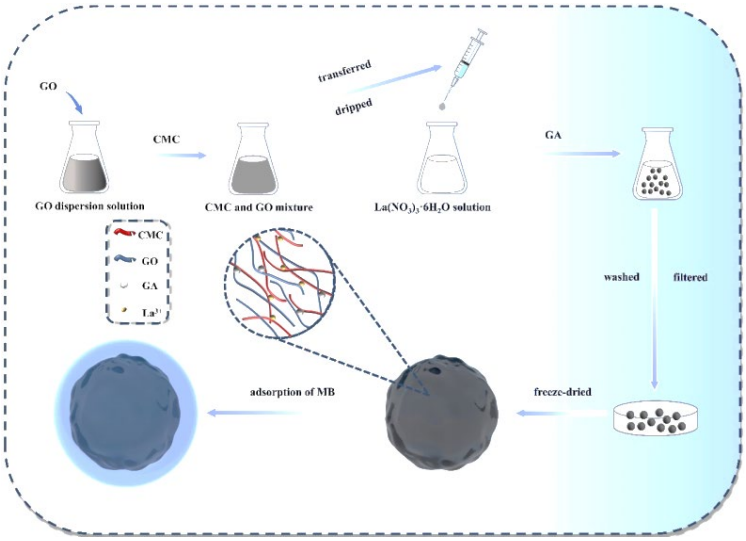

Figure 1: Schematic illustration of the crosslinking and formation process of CMC-GA-La-GO

Material characterizations

The chemical structures of the GO, CMC and CMC-GA-La-GO were analyzed using a Fourier-transform infrared (FTIR) spectrometer (Spotlight 200 Spectrometer, PerkinElmer Inc., Waltham, MA, USA) in the spectrum range of 800-3700 cm^{-1}. The materials were analyzed using XRD (EMPYREAM, Malvern Panalytical, Netherlands) in reflection mode in the 2θ range from 10 to 40°. TGA (STA449C, Netzsch, German) was used for thermogravimetric analysis at a temperature rise of 10 °C·min^{-1} from 30 to 780 °C under N_2 atmosphere. Sample surface morphology was examined using a double ion beam field emission scanning electron microscope (SEM, Gala3 XMN, Tescan, Brno, Czech Republic). The surface area and pore structure parameters were determined by nitrogen adsorption-desorption measurements using a surface area and porosity analyzer (TriStar II 3020 3.02, Micromeritics, USA). The surface chemical composition and the interactions between MB and functional groups on the adsorbent were investigated by X-ray photoelectron spectroscopy (XPS, Thermo Escalab 250Xi, USA).

Adsorption of MB

Kinetic adsorption tests were conducted using CMC-GA-La-GO (10.8 mg) with 100 mL of MB aqueous solution (10 mg·L^{-1}). The mixtures were maintained at a stable temperature of 25 °C for different durations, after which the CMC-GA-La-GO beads were separated from the solution and analyzed in order to monitor the kinetics. Additional experiments were conducted to determine parameter effects. The effect of adsorbent dosage on MB adsorption was evaluated at a constant starting concentration (10 mg·L^{-1}) and time of contact (360 h). After adsorption, a 721 visible spectrophotometer (INESA Scientific Instrument Co., Ltd., China) measured MB concentration in the residual solution at 654 nm. The following formulas were used to determine the adsorbents' adsorption capacity (q_e) and removal percentage (R%) for MB:

$$q = \frac{(C_0 - C_e)V}{m} \quad (1)$$

$$R(\%) = \frac{C_0 - C_e}{C_0} \times 100 \quad (2)$$

where C_0 and C_e (mg·L^{-1}) are the concentrations of MB before and after adsorption, respectively; V (mL) is the volume of MB solution and m (mg) is the adsorbent dosage of CMC-GA-La-GO.

RESULTS AND DISCUSSION

Characterization of CMC-GA-La-GO

The FTIR analysis of GO, as shown in Figure 2(a), revealed a broad peak at 3600-3000 cm^{-1}, which was assigned to the typical stretching vibration of -OH groups. The peak observed at 1618 cm^{-1} was assigned to aromatic skeletal C=C stretching vibrations of GO.[32] The surface of GO contains abundant oxygen-containing functional groups, as demonstrated by the characteristic peaks at 1720 cm^{-1}, 1222 cm^{-1}, and 1041 cm^{-1}. These peaks were attributed to the stretching vibration of C=O in carboxylic acid and ketone carbonyl, as well as the C-O stretching in carboxylic acid and the C-O-C stretching vibration.[33-35] In FTIR

analysis of CMC, -OH groups were observed at 3287 cm^{-1}. Distinct characteristic peaks were identified at 2823, 1506, 1357, 1260 and 996 cm^{-1}, corresponding to the stretching vibrations of C-H, -COO, O-H, and C-O, respectively.[36,37] It is worthy of note that the characteristic band of C=O was not observed in CMC. However, the adsorption band at 1725 cm^{-1} was observed in CMC-GA-La-GO, which was attributed to the stretching of C=O from GO.[29] Furthermore, a comparison of the spectra revealed that the stretching vibration of the -OH group in CMC-GA-La-GO was observed at 3349 cm^{-1}, while in GO it was observed at 3245 cm^{-1} and in CMC at 3239 cm^{-1}. The observed shift in the -OH stretching vibration suggested the successful occurrence of the crosslinking.[38]

The XRD patterns of the CMC, GO, and CMC-GA-La-GO in the region 5-80° are depicted in Figure 2(b). The diffraction peak at 15.13° in CMC is indicative of its semi-crystalline structure.[39] It was observed that the plane diffraction peak of GO was located at 11.52°, whereas the diffraction peak of CMC-GA-La-GO was located at 12.39°. The shift in the diffraction peak of the CMC-GA-La-GO indicated that the functionalization of GO with CMC was successful.[40,41]

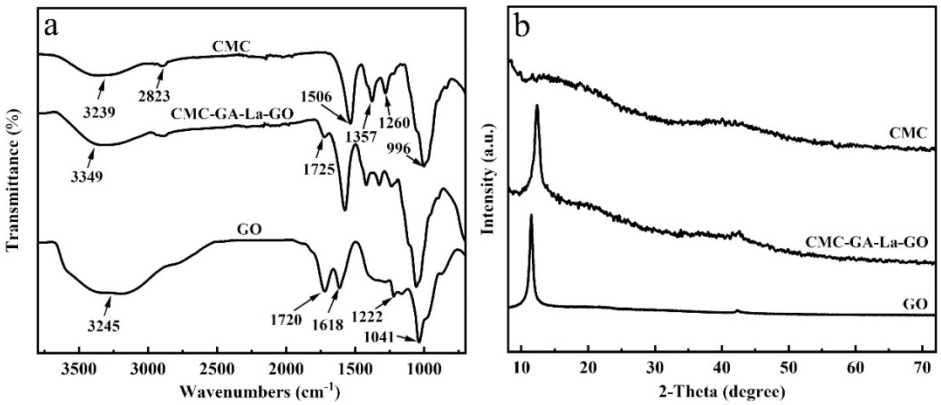

Figure 2: (a) FTIR spectra, and (b) XRD patterns of CMC, GO and CMC-GA-La-GO

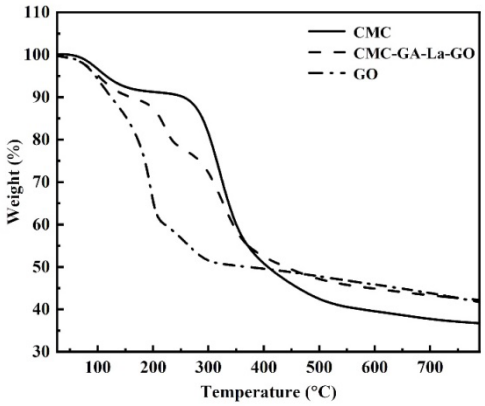

Figure 3: TGA curves of CMC, GO and CMC-GA-La-GO

The results of the TGA conducted on CMC, GO, and CMC-GA-La-GO are presented in Figure 3. As a result of physical adsorption of water, all samples lost weight when heated up to 100 °C.[42] A weight loss of 7.0% was observed for CMC during temperatures ranging from 100 up to 260 °C. This loss was attributed to the decomposition of the polysaccharide hydrocarbon backbone, which resulted in the release of CO_2.[43] Finally, CMC exhibited substantial mass loss, reaching approximately 51.9% in the temperature range of 260 to 600 °C The rate of weight loss for CMC exhibited a notable decline and subsequent deceleration, potentially indicating the decomposition of its lattice structure, as evidenced by the attainment of its maximum weight loss value.[44] For GO, the mass loss was 42.8% between 100 and 300 °C, mainly due to the thermal decomposition of unstable oxygen-containing functional groups.

Figure 3 shows the three primary weight reduction processes for CMC-GA-La-GO. The

initial weight loss was observed to occur in the temperature range of 100 to 250 °C, linked to the dehydration of saccharide rings, the cleavage of C-O-C bonds in CMC, and the decomposition of polymer main chains.[45] The second phase of weight reduction occurred between 250 and 380 °C, which was attributed to the thermal degradation of GO and the ensuing decomposition and carbonization of CMC. At 380 to 800 °C, weight loss reached the third stage, attributed to residual polymer degradation.[46] The residual carbon content of CMC and CMC-GA-La-GO was 36.7 and 42.2%, respectively, after heating to 800 °C. According to this, the thermal stability of the CMC-GA-La-GO was significantly improved by incorporation of GO. The enhanced crosslinked structure was identified as the underlying cause of the increased thermal stability of the prepared adsorbents.[47]

The morphologies of the CMC and CMC-GA-La-GO were investigated by SEM. Figure 4(a-f) shows that both adsorbents exhibited numerous surface wrinkles, which increased the surface area available for ion adsorption.[30] The surface of CMC-GA-La-GO had rougher wrinkles. Figure 4(g-l) displayed a cross-sectional image of the CMC and CMC-GA-La-GO, revealing that both adsorbents possessed a three-dimensional network structure. However, the CMC-GA-La-GO exhibited a more folded and uneven surface as a consequence of the presence of GO, which had the potential to significantly enhance the adsorption capacity.[10]

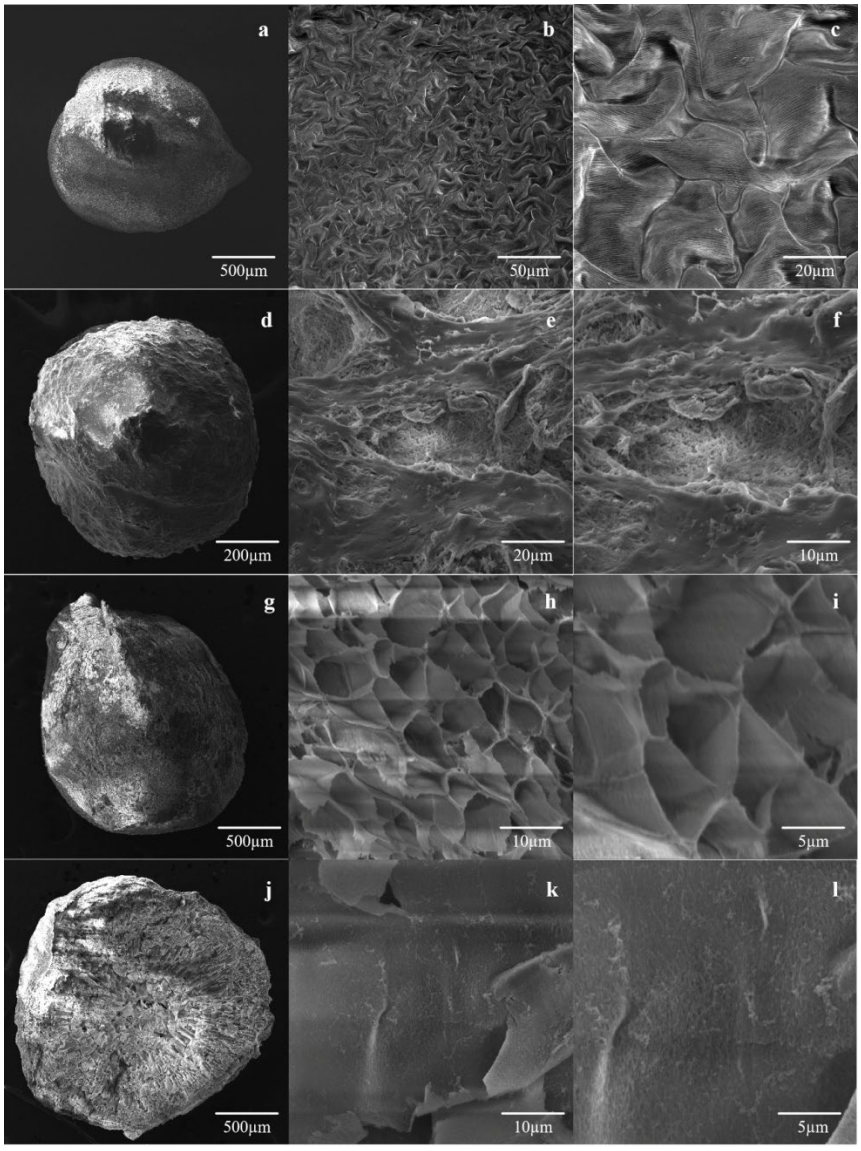

Figure 4: Surface (a-f) and cross-section (g-l) SEM images of CMC and CMC-GA-La-GO

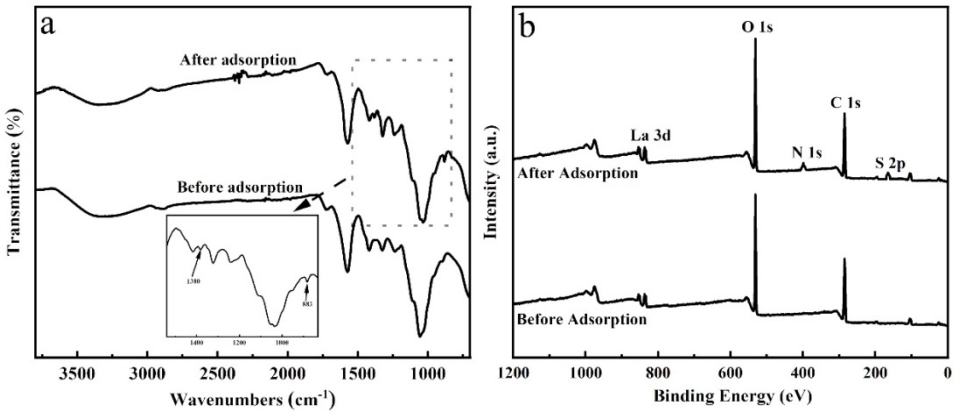

Figure 5: (a) FTIR spectra of CMC-GA-La-GO before and after MB adsorption; (b) XPS spectra of the adsorbent before and after MB adsorption

The specific surface area and porosity of the CMC-GA-La-GO adsorbent were characterized using nitrogen adsorption-desorption analysis. Through this analysis, the Brunauer-Emmett-Teller (BET) surface area was determined to be 10.60 $m^2 \cdot g^{-1}$, while the total pore volume was measured as 0.70 $cm^3 \cdot g^{-1}$ and the average pore diameter was calculated to be 40.61 nm. The pore structure with an average diameter of 40.61 nm was considered to provide favorable conditions for the diffusion of MB molecules into the internal structure of the adsorbent. Although the specific surface area of the adsorbent was found to be relatively low, high adsorption capacity was demonstrated in this study. This observation suggested that chemisorption, mediated by the abundant functional groups present on both CMC and GO, played a more dominant role in the adsorption process than physical surface area-dependent adsorption.

Adsorption performance

Adsorption kinetics

Figure 6 illustrates that the adsorption of MB onto the adsorbents was affected by contact time. During the initial stage of adsorption, the adsorbent capacity increased rapidly, subsequently followed by a gradual decrease in the pace of adsorption as the reactive sites became saturated. The adsorption rate attained dynamic equilibrium after 336 h, with a removal rate of 95.9%. The adsorption was attributed to the availability of active sites on the surface of the adsorbent. As these sites were gradually occupied, the adsorption efficiency decreased.[48-50] Herein, the interaction period of 336 h was adequate to observe the saturated adsorption capacity of the adsorbent.[51] The results showed that the incorporation of GO markedly enhanced the adsorption of MB dye relative to the native CMC.

The adsorption characteristics of CMC-GA-La-GO in the MB solution were analyzed by the pseudo-first-order and pseudo-second-order kinetic models. The linear representation of kinetics was articulated as follows:

Pseudo-first-order: $$\frac{1}{q_t} = \frac{k_1}{q_e t} + \frac{1}{q_e} \quad (3)$$

Pseudo-second-order: $$\frac{t}{q_t} = \frac{t}{q_e} + \frac{1}{k_2 q_e^2} \quad (4)$$

where q_t and q_e ($mg \cdot g^{-1}$) are the MB uptake at time t and at equilibrium, respectively; k_1 (h^{-1}) and k_2 ($g \cdot mg^{-1} \cdot h^{-1}$) represent the rate constants of the pseudo-first-order and pseudo-second-order kinetic models, respectively.

Furthermore, the intra-particle diffusion model was applied to provide an in-depth interpretation of the diffusion mechanism. The linear equation is expressed as:

Intra-particle diffusion: $$q_t = k_{ip} \cdot t^{\frac{1}{2}} + C \quad (5)$$

where q_t ($mg \cdot g^{-1}$) is adsorption capacity at time t (h); k_{ip} ($mg \cdot g^{-1} \cdot min^{-0.5}$) is the rate constant of the intra-particle diffusion model and C is the boundary layer constant.

Figure 7(a-b) shows that the adsorption of MB onto the CMC-GA-La-GO was fitted linearly by both the pseudo-first-order and pseudo-second-order kinetic models. The kinetic parameters were presented in Table 1. The pseudo-second-order model demonstrated superior alignment with the experimental data compared to the pseudo-first-order model, as indicated by the elevated correlation coefficient R^2 (refer to Table 1). These results suggested that the adsorption process of the CMC-GA-La-GO for MB was controlled by

chemisorption. Consequently, the adsorption process was accurately described by the pseudo-second-order model.

As shown in Figure 8, the adsorption process was characterized by three distinct diffusion stages. The corresponding dynamic parameters are listed in Table 2. The first stage (0-48 h) was attributed to instantaneous surface adsorption and the diffusion of MB molecules through the boundary layer to the external surface of the adsorbent.

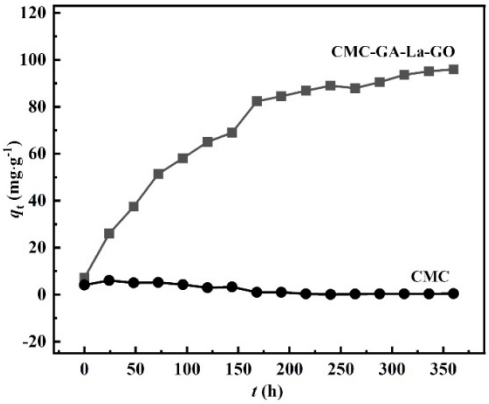

Figure 6: Effect of contact time on adsorption of MB onto CMC-GA-La-GO

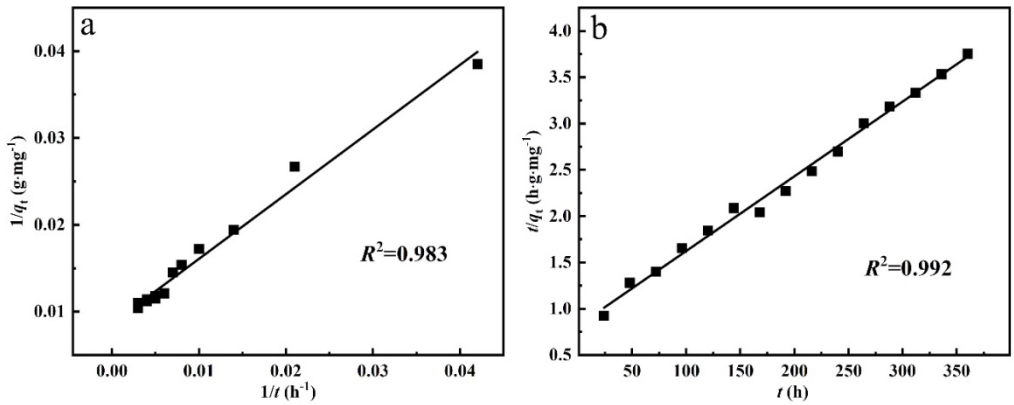

Figure 7: Adsorption kinetics of MB adsorbed by CMC-GA-La-GO: (a) pseudo-first-order model; (b) pseudo-second-order model

Table 1
Kinetic parameters obtained from pseudo-first-order and pseudo-second-order kinetic models for MB removal by CMC-GA-La-GO

Adsorbent	Pseudo-first-order			Pseudo-second-order		
	k_1 (h^{-1})	q_e (mg·g^{-1})	R^2	k_2 (g·mg^{-1}·h^{-1})	q_e (mg·g^{-1})	R^2
CMC-GA-La-GO	86.31004	115.9	0.983	0.00008	124.0	0.992

The second stage (72-144 h) was identified as the gradual intra-particle diffusion model phase, where MB molecules were transported through the internal structure of the CMC-GA-La-GO. This stage was determined to be the rate-limiting step due to the significant diffusion resistance imposed by the dual-crosslinked network. The third stage (168-360 h) corresponded to the final equilibrium phase, where the adsorption sites were largely saturated and the diffusion rate was substantially diminished.[52] Furthermore, it was observed that the fitted lines for all stages did not pass through the origin ($C \neq 0$), indicating that the intra-particle diffusion model was not the exclusive rate-controlling mechanism and that boundary layer diffusion also played a significant role throughout the adsorption process.[53]

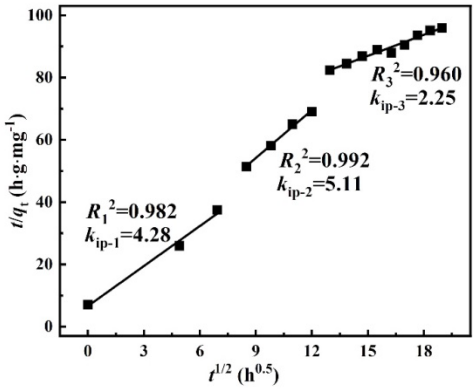

Figure 8: Intra-particle diffusion model for the adsorption of MB onto the CMC-GA-La-GO

Table 2
Kinetic parameters obtained from intra-particle diffusion model for MB removal by CMC-GA-La-GO

Adsorbent	Intra-particle diffusion model					
	k_{ip-1} (mg·g^{-1}·h$^{-0.5}$)	k_{ip-2} (mg·g^{-1}·h$^{-0.5}$)	k_{ip-3} (mg·g^{-1}·h$^{-0.5}$)	R_1^2	R_2^2	R_3^2
CMC-GA-La-GO	4.28	5.11	2.25	0.982	0.992	0.960

Effect of adsorbent dosage on the adsorption capacity

Figure 9(a) illustrates the influence of the adsorbent dosage on the adsorption capability of CMC-GA-La-GO for MB. The removal percentage rose from 87.1% to 99.9% as the adsorbent dosage escalated from 2.1 to 20.0 mg. The rise in removal percentage was correlated with a reduction in capacity for adsorption from 137.4 to 24.2 mg·g^{-1}. At a minimal adsorbent dosage, the adsorption sites became saturated due to the adsorption of MB. With increasing adsorbent dosage, the available adsorption sites per unit mass decreased, leading to reduced adsorption capacity.[54,55] Consequently, after a thorough evaluation of the adsorption ability of CMC-GA-La-GO and the removal percentage of MB, 6 mg of CMC-GA-La-GO was selected as the optimal dosage for subsequent adsorption studies.

Adsorption isotherm

Adsorption isotherm models were utilized to examine the adsorption efficacy of CMC-GA-La-GO and to analyze the interactions between the adsorbent and the adsorbate, which was apparent in Figure 9(b). The Langmuir model describes saturated monolayer adsorption on the adsorbent,[56,57] while the Freundlich model is an empirical equation for heterogeneous adsorption.[58,59] The linear equations are expressed as:

Langmuir isotherm model: $$\frac{C_e}{q_e} = \frac{C_e}{q_m} + \frac{1}{K_L q_m} \quad (6)$$

Freundlich isotherm model:

$$\ln q_e = \ln K_F + \frac{1}{n} \ln C_e \quad (7)$$

where C_e (mg·L^{-1}), q_e (mg·g^{-1}) and q_m (mg·g^{-1}) are the equilibrium concentration, equilibrium adsorption capacity and theoretical maximum adsorption capacity, respectively. K_L (L·mg^{-1}) is the Langmuir constant; K_F (mg^{1-n}·L^n·g^{-1}) is the Freundlich constant and n is the dimensionless constant.

Table 3 provides a summary of the isotherm parameters and determination coefficients. The R^2 value derived from fitting the Langmuir model demonstrated superior alignment with the experimental data, compared to the Freundlich model, indicating that the Langmuir model characterizes better the adsorption process, suggesting monolayer adsorption of MB onto CMC-GA-La-GO.

Effect of temperature on the adsorption capacity

The effect of temperature on the adsorption capacity of methylene blue onto the CMC-GA-La-GO was systematically investigated over a range from 25 to 50 °C. As shown in Figure 10a, the adsorption capacity was observed to decrease continuously from 95.92 mg·g^{-1} to 22.72 mg·g^{-1} with increasing temperature. This trend is

consistent with the characteristics of an exothermic adsorption process. The diminished adsorption at elevated temperatures suggests that the binding interactions between MB molecules and the active sites of the adsorbent were weakened by the increased thermal energy.[44]

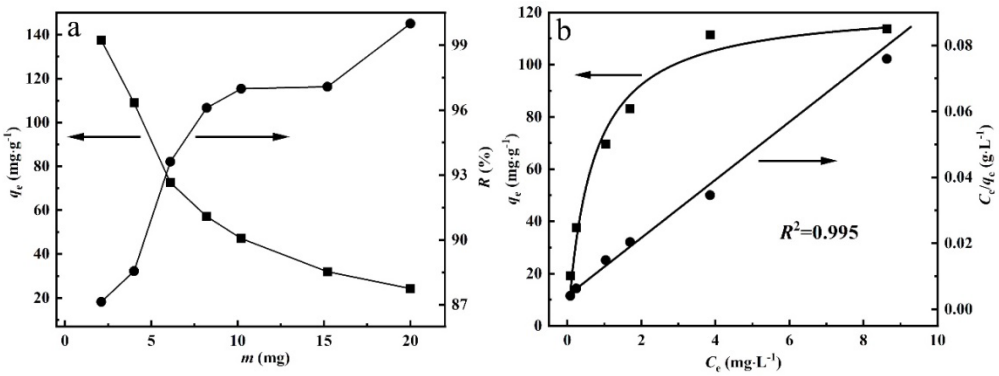

Figure 9: (a) Effects of the adsorbent dosage on the adsorption capacity and the removal percentage for MB; (b) Langmuir adsorption isotherm and Langmuir linear fit for the adsorption of MB onto CMC-GA-La-GO

Table 3
Isotherm constants and correlation coefficients for MB adsorption onto CMC-GA-La-GO

Model	Langmuir			Freundlich		
	q_m (mg·g^{-1})	K_L (L·mg^{-1})	R^2	K_F (L·g^{-1})	n	R^2
	113.9	2.12	0.995	60.92	2.56	0.923

Effect of pH on the adsorption capacity

The effect of initial solution pH on the adsorption capacity of MB was investigated over a pH range of 1-10. As shown in Figure 10(b), the adsorption capacity increased progressively from pH 1 to 8. However, a slight decrease was observed when the pH was further increased to 10. The initial increase could be attributed to the enhanced electrostatic attraction between the negatively charged adsorbent surface and the cationic MB molecules, resulting from the deprotonation of oxygen-containing functional groups under higher pH conditions.[60] The subsequent decline under strongly alkaline conditions might be caused by the structural deformation of the adsorbent material in extreme pH environments.[44]

Table 4 presents a comparison of the adsorption capacity of MB between CMC-GA-La-GO and other adsorbents documented in the literature. It can be observed that CMC-GA-La-GO exhibits a greater adsorption capacity for MB in comparison with numerous adsorbents documented in the existing literature. However, it was noteworthy that higher adsorption capacities have been demonstrated by some adsorbents. For instance, the optimal oxidized weeds-based biochar (OWC) treated with concentrated HNO_3 was reported by Güzel *et al*. to have achieved an adsorption capacity of 161.29 mg·g^{-1}, though extensive acid treatment was involved in this preparation process.[61] Similarly, while adsorbents such as magnetic alginate-functionalized multiwalled carbon nanotube beads (A-F-Fe_2O_3) and magnetic metal-organic frameworks (Fe_3O_4@AMCA-MIL-53(Al)) have demonstrated exceptionally high adsorption capacities of 905.5 mg·g^{-1} and 325.62 mg·g^{-1} respectively, their practical implementation faced common limitations. These included the relatively high material costs, complex synthesis procedures, and potential environmental concerns associated with the utilization of engineered nanomaterials in large-scale water treatment applications.[62,63] In comparison, the CMC-GA-La-GO beads fabricated in this study were synthesized via a more environmentally friendly route without requiring harsh chemicals or complex procedures, while still maintaining favorable adsorption capacity and macroscopic integrity, conducive to practical separation processes.

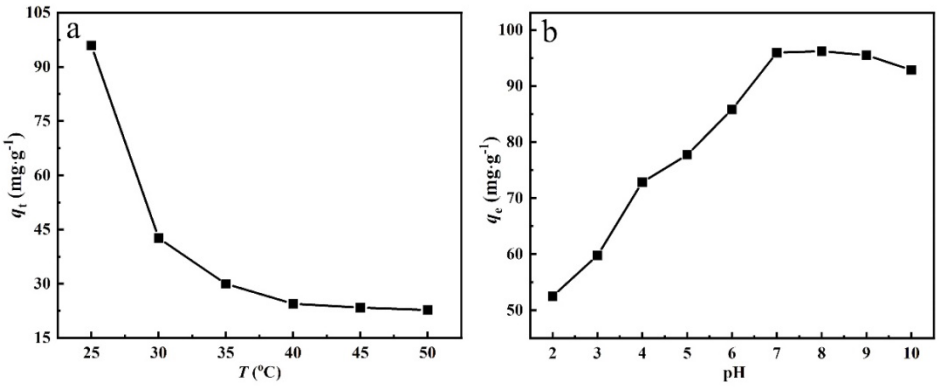

Figure 10: Effects of temperature (a) and (b) pH on the adsorption capacity

Table 4
Comparison of the maximum adsorption of MB onto diverse adsorbents

Adsorbents	q_m (mg·g^{-1})	Ref.
CMC-GA-La-GO	113.9	This work
Fe_3O_4@PDA/HKUST-1	34.0	[64]
CMC/kC/AMMT composite beads	12.25	[20]
IP	17.0	[65]
XG5	26.04	[66]
Biomass fly ash geopolymer monoliths	20.5	[67]
OWC	161.29	[61]
A-F-Fe_2O_3 beads	905.5	[62]
Fe_3O_4@AMCA-MIL-53(Al)	325.62	[63]

The chemical states of the CMC-GA-La-GO before and after MB adsorption were characterized by FTIR and XPS. As shown in Figure 5a, new peaks at 883 cm^{-1} and 1380 cm^{-1} appeared after adsorption, which were assigned to the aromatic ring skeleton vibration and the C-N stretching vibration of MB molecules, respectively. The decreased intensity of the -OH stretching band and shifts in characteristic peaks suggested the involvement of hydrogen bonding and chemical interactions between oxygen-containing functional groups.

The XPS analysis provided further evidence for the successful adsorption of MB. As shown in Figure 5b, new peaks corresponding to N 1s (399.78 eV) and S 2p (164.33 eV) emerged in the spectrum of the adsorbent after adsorption, confirming the successful adsorption of MB molecules onto the adsorbent. These results collectively demonstrate that the adsorption mechanism involved multiple interactions, including electrostatic attraction between the negatively charged adsorbent surface and cationic MB, and chemical interactions involving oxygen-containing functional groups.

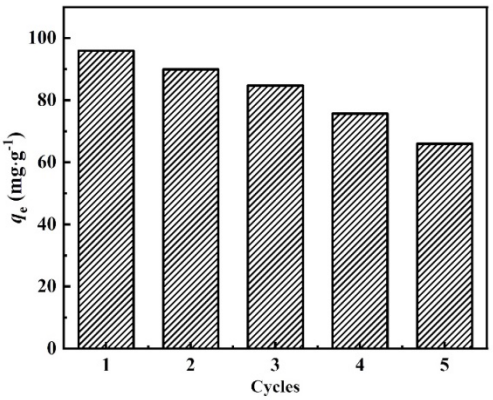

Figure 11: Adsorption-desorption cycles of CMC-GA-La-GO for MB

Adsorbent regeneration

The desorption and reusability of the CMC-GA-La-GO adsorbent were evaluated over five consecutive adsorption-desorption cycles. The desorption process was carried out using 0.1 $mol \cdot L^{-1}$ HCl solution, which was selected based on the pH-dependent adsorption results (Fig. 10b). The adsorption capacity decreased from an initial 95.93 $mg \cdot g^{-1}$ to 66.02 $mg \cdot g^{-1}$ after five cycles. This reduction in adsorption capacity might be attributed to either the incomplete desorption of MB molecules that remained bound to active sites, or to potential structural alterations of the adsorbent induced by prolonged exposure to the acidic environment during the desorption process.[62]

CONCLUSION

In conclusion, an adsorbent (CMC-GA-La-GO) was successfully fabricated through a novel dual-crosslinking strategy. The CMC-GA-La-GO synthesis process was a straightforward and environmentally benign method that did not require the use of heating. This approach effectively avoided the wastage of resources, thus representing a highly efficient and cost-effective solution. Moreover, the raw materials were inexpensive and readily available, resulting in a considerable reduction in fabrication costs. The framework, formed by synergistic ionic crosslinking with La^{3+} and covalent crosslinking with GA, effectively incorporates GO into the CMC network and mitigates its restacking. This unique structure confers excellent stability to the composite throughout the prolonged adsorption period and a high removal efficiency of nearly 100% for MB from a dilute solution. The data further demonstrated that the adsorption with MB onto the adsorbent composite surface was more compatible with the Langmuir isotherm. The produced adsorbent was shown to have a theoretical maximum adsorption capacity of 113.9 $mg \cdot g^{-1}$. The adsorption process followed the pseudo-second-order kinetic model. Therefore, CMC-GA-La-GO beads are efficient and beneficial as adsorbents for removing cationic dyes and have the potential to be used in environmental remediation.

ACKNOWLEDGMENTS: This work was supported by National Natural Science Foundation of China (NNSFC, No. 11965015), Program for Young Talents of Science and Technology in Universities of Inner Mongolia Autonomous Region (No. NJYT22072), Fundamental Research Funds for Inner Mongolia University of Science and Technology, Inner Mongolia "Grassland Talents" Special Research Project and Inner Mongolia Talent Development Fund.

REFERENCES

[1] R. P. Schwarzenbach, B. I. Escher, K. Fenner, T. B. Hofstetter, C. A. Johnson *et al*., *Science*, **313**, 1072 (2006), http://dx.doi.org/10.1126/science.1127291

[2] A. Cruz-Rizo, S. Gutiérrez-Granados, R. Salazar and J. M. Peralta-Hernández, *Separ. Purif. Technol*., **172**, 296 (2017), http://dx.doi.org/10.1016/j.seppur.2016.08.029

[3] J. Zhao, Z. Lu, X. He, X. Zhang, Q. Li *et al*., *ACS Sustain. Chem. Eng*., **5**, 7723 (2017), http://dx.doi.org/10.1021/acssuschemeng.7b01175

[4] E. D. D. Melo, A. H. Mounteer, L. H. D. S. Leão, R. C. B. Bahia and I. M. F. Campos, *J. Hazard. Mater*., **244-245**, 329 (2013), http://dx.doi.org/10.1016/j.jhazmat.2012.11.051

[5] A. A. Mohana, S. M. Farhad, N. Haque and B. K. Pramanik, *Chemosphere*, **284**, 131430 (2021), http://dx.doi.org/10.1016/j.chemosphere.2021.131430

[6] M. Shahid, I. Shahid and F. Mohammad, *J. Clean. Prod*., **53**, 310 (2013), http://dx.doi.org/10.1016/j.jclepro.2013.03.031

[7] Inamuddin, *Int. J. Biol. Macromol*., **121**, 1046 (2019), http://dx.doi.org/10.1016/j.ijbiomac.2018.10.064

[8] I. Khan, M. Usman, M. Imran and K. Saeed, *J. Mater. Sci.*: *Mater. Electron*., **31**, 8971 (2020), http://dx.doi.org/10.1007/s10854-020-03431-6

[9] M. Contreras, C. D. Grande-Tovar, W. Vallejo and C. Chaves-López, *Water*, **11** (2019), http://dx.doi.org/10.3390/w11020282

[10] E. N. Mohamed, A. I. Abd-Elhamid, A. A. El-Bardan, H. M. A. Soliman and M. S. Mohy-Eldin, *Sci. Rep*., **13**, 14265 (2023), http://dx.doi.org/10.1038/s41598-023-41431-8

[11] P. O. Oladoye, T. O. Ajiboye, E. O. Omotola and O. J. Oyewola, *Results Eng*., **16**, 100678 (2022), http://dx.doi.org/10.1016/j.rineng.2022.100678

[12] S. Shakoor and A. Nasar, *Groundwater Sustain. Develop*., **5**, 152 (2017), http://dx.doi.org/10.1016/j.gsd.2017.06.005

[13] A. Zuorro and R. Lavecchia, *Desalin. Water Treat*., **52**, 1571 (2014), http://dx.doi.org/10.1080/19443994.2013.787553

[14] A. Khataee, G. Dehghan, M. Zarei, S. Fallah, G. Niaei *et al*., *Chem. Ecol*., **29**, 221 (2013), http://dx.doi.org/10.1080/02757540.2012.744831

[15] Z. Aksu, S. Ertuğrul and G. Dönmez, *Chem. Eng. J*., **158**, 474 (2010), http://dx.doi.org/10.1016/j.cej.2010.01.029

[16] L. Liu, Z. Y. Gao, X. P. Su, X. Chen, L. Jiang *et al*., *ACS Sustain. Chem. Eng*., **3**, 432 (2015), http://dx.doi.org/10.1021/sc500848m
[17] S. Chatterjee, D. S. Lee, M. W. Lee and S. H. Woo, *Bioresour. Technol*., **100**, 2803 (2009), http://dx.doi.org/10.1016/j.biortech.2008.12.035
[18] A. Dong, J. Xie, W. Wang, L. Yu, Q. Liu *et al*., *J. Hazard. Mater*., **181**, 448 (2010), http://dx.doi.org/10.1016/j.jhazmat.2010.05.031
[19] N. Fattahi, T. Fattahi, M. Kashif, A. Ramazani and W.-K. Jung, *Int. J. Biol. Macromol*., **276**, 133763 (2024), http://dx.doi.org/10.1016/j.ijbiomac.2024.133763
[20] C. Liu, A. M. Omer and X.-K. Ouyang, *Int. J. Biol. Macromol*., **106**, 823 (2018), http://dx.doi.org/10.1016/j.ijbiomac.2017.08.084
[21] Z. Sun, Y. Yin, Y. An, C. Deng, Z. Wei *et al*., *J. Environ. Chem. Eng*., **10**, 108179 (2022), http://dx.doi.org/10.1016/j.jece.2022.108179
[22] G. Zhang, L. Yi, H. Deng and P. Sun, *J. Environ. Sci*., **26**, 1203 (2014), http://dx.doi.org/10.1016/S1001-0742(13)60513-6
[23] M. Yadollahi, I. Gholamali, H. Namazi and M. Aghazadeh, *Int. J. Biol. Macromol*., **74**, 136 (2015), http://dx.doi.org/10.1016/j.ijbiomac.2014.11.032
[24] W. Konicki, M. Aleksandrzak, D. Moszyński and E. Mijowska, *J. Colloid Interface Sci*., **496**, 188 (2017), http://dx.doi.org/10.1016/j.jcis.2017.02.031
[25] Y. Yang, S. Song and Z. Zhao, *Colloids Surfaces A: Physicochem. Eng. Aspects*, **513**, 315 (2017), http://dx.doi.org/10.1016/j.colsurfa.2016.10.060
[26] J. Liu, H. Chu, H. Wei, H. Zhu, G. Wang *et al*., *RSC Adv*., **6**, 50061 (2016), http://dx.doi.org/10.1039/C6RA06438H
[27] V. H. Luan, H. N. Tien and S. H. Hur, *J. Colloid Interface Sci*., **437**, 181 (2015), http://dx.doi.org/10.1016/j.jcis.2014.08.071
[28] Y.-C. Shi, A.-J. Wang, X.-L. Wu, J.-R. Chen and J.-J. Feng, *J. Colloid Interface Sci*., **484**, 254 (2016), http://dx.doi.org/10.1016/j.jcis.2016.09.008
[29] X. He, L. Zeng, X. Cheng, C. Yang, J. Chen *et al*., *Eur. Polym. J*., **156**, 110592 (2021), http://dx.doi.org/10.1016/j.eurpolymj.2021.110592
[30] J. Wang, X. Lin, X. Luo and W. Yao, *RSC Adv*., **5**, 59273 (2015), http://dx.doi.org/10.1039/C5RA07024D
[31] Q. Peng, T. Jin, C. Wang and Y. Qian, *Int. J. Biol. Macromol*., **256**, 128545 (2024), http://dx.doi.org/https://doi.org/10.1016/j.ijbiomac.2023.128545
[32] T. A. Saleh, A. Sarı and M. Tuzen, *Chem. Eng. J*., **307**, 230 (2017), http://dx.doi.org/10.1016/j.cej.2016.08.070
[33] Q. Xu, M. Zeng, Z. Feng, D. Yin, Y. Huang *et al*., *RSC Adv*., **6**, 31484 (2016), http://dx.doi.org/10.1039/C5RA28016H
[34] S. Sharma and N. C. Kothiyal, *RSC Adv*., **5**, 52642 (2015), http://dx.doi.org/10.1039/C5RA08078A
[35] Y. Hao, Y. Cui, J. Peng, N. Zhao, S. Li *et al*., *Carbohyd. Polym*., **208**, 269 (2019), http://dx.doi.org/10.1016/j.carbpol.2018.12.068
[36] M. J. Zohuriaan-Mehr, A. Pourjavadi and M. Salehi-Rad, *React. Funct. Polym*., **61**, 23 (2004), http://dx.doi.org/10.1016/j.reactfunctpolym.2004.03.006
[37] X. Ge, Y. Shan, L. Wu, X. Mu, H. Peng *et al*., *Carbohyd. Polym*., **197**, 277 (2018), http://dx.doi.org/10.1016/j.carbpol.2018.06.014
[38] H. Liu, X. Tian, X. Xiang and S. Chen, *Int. J. Biol. Macromol*., **202**, 632 (2022), http://dx.doi.org/10.1016/j.ijbiomac.2022.01.052
[39] Y. Zhang, Y. Liu, X. Wang, Z. Sun, J. Ma *et al*., *Carbohyd. Polym*., **101**, 392 (2014), http://dx.doi.org/10.1016/j.carbpol.2013.09.066
[40] H. Mittal, A. Al Alili, P. P. Morajkar and S. M. Alhassan, *Int. J. Biol. Macromol*., **167**, 1248 (2021), http://dx.doi.org/10.1016/j.ijbiomac.2020.11.079
[41] H.-A. S. Tohamy, M. El-Sakhawy and S. Kamel, *J. Polym. Environ*., **29**, 859 (2021), http://dx.doi.org/10.1007/s10924-020-01920-7
[42] A. I. Abd-Elhamid, E. M. Abu Elgoud and H. F. Aly, *Cellulose*, **29**, 9831 (2022), http://dx.doi.org/10.1007/s10570-022-04862-6
[43] N. A. Dahlan, J. Pushpamalar, A. K. Veeramachineni and S. Muniyandy, *J. Polym. Environ*., **26**, 2061 (2018), http://dx.doi.org/10.1007/s10924-017-1105-3
[44] A. S. Eltaweil, G. S. Elgarhy, G. M. El-Subruiti and A. M. Omer, *Int. J. Biol. Macromol*., **154**, 307 (2020), http://dx.doi.org/https://doi.org/10.1016/j.ijbiomac.2020.03.122
[45] Z. Wang, A. Ning, P. Xie, G. Gao, L. Xie *et al*., *Carbohyd. Polym*., **157**, 48 (2017), http://dx.doi.org/10.1016/j.carbpol.2016.09.070
[46] Y. Hao, J. Qu, L. Tan, Z. Liu, Y. Wang *et al*., *Int. J. Biol. Macromol*., **233**, 123643 (2023), http://dx.doi.org/10.1016/j.ijbiomac.2023.123643
[47] Y. Guo, B. Duan, L. Cui and P. Zhu, *Cellulose*, **22**, 2035 (2015), http://dx.doi.org/10.1007/s10570-015-0630-2
[48] A. Abd-Elhamid, A. Nayl, A. A. E. Shanshory, H. M. Soliman and H. J. R. A. Aly, *RSC Adv*., **9**, 5770 (2019), http://dx.doi.org/10.1039/C8RA10449B
[49] A. Saeed, M. Sharif and M. Iqbal, *J. Hazard. Mater*., **179**, 564 (2010), http://dx.doi.org/10.1016/j.jhazmat.2010.03.041
[50] E. Errais, J. Duplay, F. Darragi, I. M'Rabet, A. Aubert *et al*., *Desalination*, **275**, 74 (2011), http://dx.doi.org/10.1016/j.desal.2011.02.031
[51] B. K. Preetha and B Vishalakshi, *J. Environ. Chem. Eng*., **8**, 103608 (2020), http://dx.doi.org/10.1016/j.jece.2019.103608
[52] H. Hosseini, A. Zirakjou, D. J. McClements, V. Goodarzi and W.-H. Chen, *J. Hazard. Mater*., **421**, 126752 (2022), http://dx.doi.org/https://doi.org/10.1016/j.jhazmat.2021.126752
[53] G. K. Ramesha, A. Vijaya Kumara, H. B. Muralidhara and S. Sampath, *J. Colloid Interface Sci*., **361**, 270 (2011),

http://dx.doi.org/https://doi.org/10.1016/j.jcis.2011.05.050
[54] F. Ren, Z. Li, W.-Z. Tan, X.-H. Liu, Z.-F. Sun *et al*., *J. Colloid Interface Sci*., **532**, 58 (2018), http://dx.doi.org/10.1016/j.jcis.2018.07.101
[55] A. Verma, S. Thakur, G. Mamba, R. K. Gupta, P. Thakur *et al*., *Int. J. Biol. Macromol*., **148**, 1130 (2020), http://dx.doi.org/10.1016/j.ijbiomac.2020.01.142
[56] Y. Zhu, Y. Zheng and A. Wang, *Int. J. Biol. Macromol*., **72**, 410 (2015), http://dx.doi.org/10.1016/j.ijbiomac.2014.08.039
[57] S. Saber-Samandari, S. Saber-Samandari, H. Joneidi-Yekta and M. Mohseni, *Appl. Surface Sci*., **308**, 1133 (2017), http://dx.doi.org/10.1016/j.cej.2016.10.017
[58] Y. Yan, Q. An, Z. Xiao, W. Zheng and S. Zhai, *Chem. Eng. J*., **313**, 475 (2017), http://dx.doi.org/10.1016/j.cej.2016.12.099
[59] Y. Kong, Y. Zhuang, Z. Han, J. Yu, B. Shi *et al*., *J. Environ. Sci*., **78**, 81 (2019), http://dx.doi.org/10.1016/j.jes.2018.07.006
[60] F. Shakib, A. Dadvand Koohi and A. Kamran Pirzaman, *Water Sci. Technol*., **75**, 1932 (2017), http://dx.doi.org/10.2166/wst.2017.077
[61] F. Güzel, H. Sayğılı, G. Akkaya Sayğılı, F. Koyuncu and C. Yılmaz, *J. Clean. Prod*., **144**, 260 (2017), http://dx.doi.org/https://doi.org/10.1016/j.jclepro.2017.01.029
[62] N. Boukhalfa, M. Boutahala, N. Djebri and A. Idris, *J. Mol. Liquids*, **275**, 431 (2019), http://dx.doi.org/https://doi.org/10.1016/j.molliq.2018.11.064
[63] A. A. Alqadami, M. Naushad, Z. A. Alothman and T. Ahamad, *J. Environ. Manag*., **223**, 29 (2018), http://dx.doi.org/https://doi.org/10.1016/j.jenvman.2018.05.090
[64] G. Zhou, Q. Wang, R. Song, S. Li, S. Yang *et al*., *J. Phys. Chem. Solids*, **172**, 111094 (2023), http://dx.doi.org/10.1016/j.jpcs.2022.111094
[65] T. Hertel, R. M. Novais, R. Murillo Alarcón, J. A. Labrincha and Y. Pontikes, *J. Clean. Prod*., **227**, 877 (2019), http://dx.doi.org/10.1016/j.jclepro.2019.04.084
[66] S. D. K. Seera, D. Kundu, P. Gami, P. K. Naik and T. Banerjee, *Carbohyd. Polym*., **256**, 117520 (2021), http://dx.doi.org/10.1016/j.carbpol.2020.117520
[67] R. M. Novais, G. Ascensão, D. M. Tobaldi, M. P. Seabra and J. A. Labrincha, *J. Clean. Prod*., **171**, 783 (2018), http://dx.doi.org/10.1016/j.jclepro.2017.10.078